Hydraulics, stomatal conductance and photosynthesis

Miquel De Cáceres[1,2]

[1]Centre Tecnològic Forestal de Catalunya. Ctra. St. Llorenç de Morunys km 2, 25280, Solsona, Catalonia, Spain
[2]CREAF, Cerdanyola del Vallès, 08193, Spain

November 15, 2017

Contents

1 Plant hydraulics

The supply-loss theory of plant hydraulics, recently presented by Sperry and Love (2015) and tested in Sperry et al. (2016a), uses the physics of flow through soil and xylem to quantify how canopy water supply declines

with drought and ceases by hydraulic failure. The theory builds on previous hydraulic model (Sperry et al. 1998) and can be applied to different ways of representing the soil-plant continuum. In our case we considered a network of $(N \times 2 + 1)$ resistance elements, with soil being represented in N different layers. For each soil layer there is a rhizosphere element in series with a root xylem element. The N different layers are in parallel up to the root crown. From there there is a final stem xylem element up to the canopy.

In Sperry and Love (2015) and Sperry et al (2016a) stomatal regulation is modelled from purely hydraulic grounds. This approach ignores the role of stomata in regulating and responding to photosynthesis (i.e., there is no trade-off between water and carbon). Sperry et al (2016b) presented a cost-benefit approach where hydraulic costs of opening the stomata are compared against photosynthetic gain. In this document we illustrate this second stomatal regulation approach using descriptions of the continuum in a network, although the simpler one-element and two-element topologies will be used in some cases to facilitate understanding. Furthermore, our examples will try to illustrate the theory under different situations comprising different soil types, soil water potentials and with/without cavitated conduits.

1.1 Xylem and rhizosphere vulnerability curves

Each continuum element has a vulnerability curve that starts at maximum hydraulic conductance (k_{max}, flow rate per pressure drop) and monotonically declines as water pressure (Ψ) becomes more negative. Vulnerability curves form the basis of the calculations.

The xylem element was assigned a two-parameter Weibull function as the vulnerability curve $k_x(\Psi)$:

$$k_x(\Psi) = k_{xmax} \cdot e^{-((\Psi/d)^c)} \tag{1}$$

where k_{xmax} is the xylem maximum hydraulic conductance (defined as flow per surface unit and per pressure drop), and c and d are species-specific parameters. For example, we define the following parameter values for a stem xylem:

```
> kstemmax = 4 # in mmol·m-2·s-1·MPa-1
> stemc = 3
> stemd = -4 # in MPa
```

For root xylem, we may assume that stem conductance represents a fixed proportion of total whole-plant conductance:

```
> ktot = kstemmax*0.625
> krootmax = 1/((1/ktot)-(1/kstemmax))
> krootmax
```

```
[1] 6.666667
```

And the root xylem is more vulnerable to cavitation:

```
> rootc = 3
> rootd = -2.5 #MPa
```

With these values, the vulnerability curves for root and stem xylem are (see `hydraulics.xylemConductance()`):

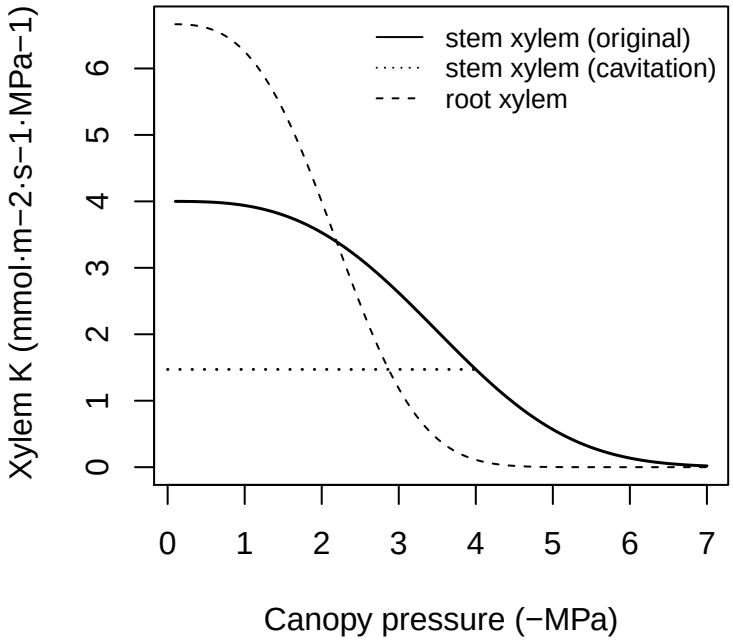

The dotted line between 0 and -4 MPa indicates the modification of the stem xylem vulnerability curve when cavitation has occurred (i.e., previous embolism limits a the maximum conductance value), as indicated in Sperry et al. (2016a). Although root xylem is more vulnerable to the formation of emboli for a given potential, it is generally accepted that the less negative potentials of root xylem compared to the stem lead to cavitation occurring more often in the stem. The constrain created by cavitation has an effect on the calculation of the flow rates and derived quantities (see section 1.2 below).

The concept of vulnerability curve can also be used to specify the relationship between pressure and conductance in any portion of the flow path along the stem or root xylem. The rhizosphere conductance function $k_r(\Psi)$ is modeled as a van Genuchten function (van Genuchten, 1980):

$$k_r(\Psi) = k_{rmax} \cdot v^{(n-1)/(2 \cdot n)} \cdot ((1-v)^{(n-1)/n} - 1)^2 \quad (2)$$

$$v = [(\alpha\Psi)^n + 1]^{-1} \quad (3)$$

where k_{rmax} is the maximum rhizosphere conductance, and n and α are texture-specific parameters (see Leij et al. 1996; Carsel & Parrish 1988). If we specify the following parameters for three soil texture types:

```
> textures = c("Sandy loam","Silt loam", "Clay")
> #Textural parameters
> #Sandy clay loam
> p1 = soil.vanGenuchtenParams(textures[1])
> p1

[1] 764.983   1.890

> alpha1 = p1[1]
> n1 = p1[2]
> #Silt loam
> p2 = soil.vanGenuchtenParams(textures[2])
> p2

[1] 203.9955   1.4100

> alpha2 =  p2[1]
> n2 = p2[2]
> #Silty clay
> p3 = soil.vanGenuchtenParams(textures[3])
> p3

[1] 81.59819  1.09000

> alpha3 =  p3[1]
> n3 = p3[2]
```

we can estimate maximum rhizosphere conductance values assuming that they account for an average percentage of the resistance (e.g. 15%) across the continuum (see functions `hydraulics.averageRhizosphereResistancePercent()` and `hydraulics.findRhizosphereMaximumConductance()`):

```
> percentResistance = 15
> #Sandy clay loam
> krmax1 = hydraulics.findRhizosphereMaximumConductance(percentResistance,
+                       n1,alpha1, krootmax, rootc,rootd, kstemmax, stemc, stemd)
> krmax1

[1] 7.148723e+14

> #Silt loam
> krmax2 = hydraulics.findRhizosphereMaximumConductance(percentResistance,
+                       n2,alpha2, krootmax, rootc,rootd, kstemmax, stemc, stemd)
> krmax2
```

```
[1] 3641367009
```

```
> #Silty clay
> krmax3 = hydraulics.findRhizosphereMaximumConductance(percentResistance,
+                         n3,alpha3, krootmax, rootc,rootd, kstemmax, stemc, stemd)
> krmax3
```

```
[1] 41088959
```

With these parameters, the resulting $k_r(\Psi)$ functions are (see `hydraulics.vanGenuchtenConductance`

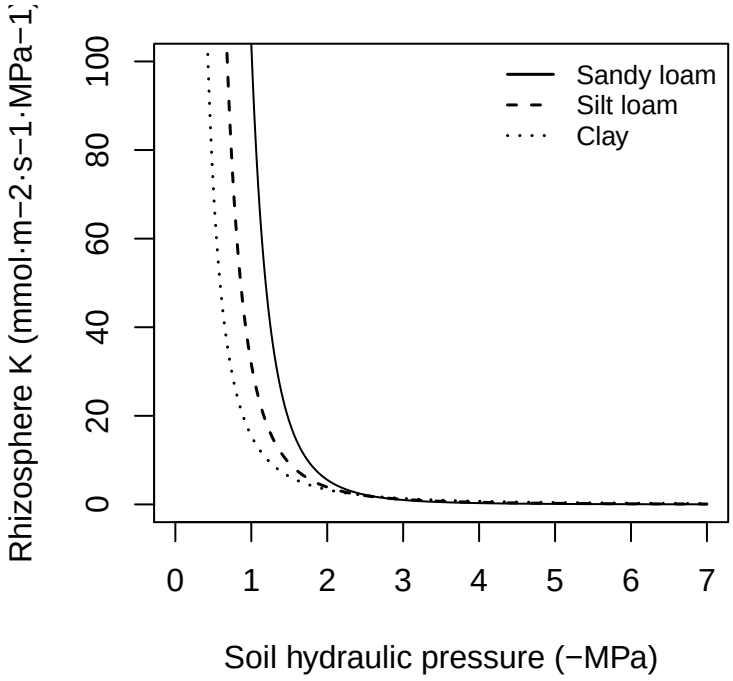

1.2 Supply functions

The supply function describes the rate of water supply (i.e. flow) for transpiration (E) as a function of pressure. The steady-state flow rate E_i through each i element of the continuum is related to the flow-induced drop in pressure across that element ($\Delta\Psi_i$) by the integral transform of the element's vulnerability curve $k_i(\Psi)$:

$$E_i(\Delta\Psi_i) = \int_{\Psi_{up}}^{\Psi_{down}} k_i(\Psi) d\Psi \tag{4}$$

where Ψ_{up} and Ψ_{down} are the upstream and downstream water potential values, respectively. The integral transform assumes infinite discretization of the flow path. The supply function can be defined for individual elements of the continuum or for the whole soil-plant continuum using different topologies. In the following subsections we illustrate the supply function for different cases.

1.2.1 Supply function for single elements

In the case of a single stem xylem element the supply function describes the flow rate as a function of canopy pressure (Ψ_{canopy}). It can be calculated by numerical integration or aproximated using an incomplete gamma function. The shape of the supply function starting at different root crown water potential values ($\Psi_{rootcrown}$) is (see `hydraulics.EXylem()`):

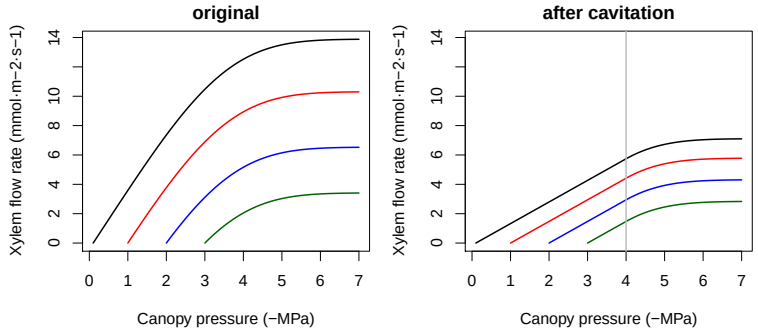

Right pane shows the supply functions that are obtained in the case of a cavitated xylem (i.e. without refilling), assuming that the minimum water potential experienced so far was -4 MPa. Note the linear part of the flow rate between Ψ_{soil} and this limit.

The supply function of the rhizosphere element relates the flow rate to the pressure inside the roots (Ψ_{root}). It is calculated by numerical integration of the van Genuchten function (see `hydraulics.E2psiVanGenuchten()`). Here we draw the supply function for the rhizosphere starting at the four different values of bulk soil pressure (Ψ_{soil}) and for the same three texture types:

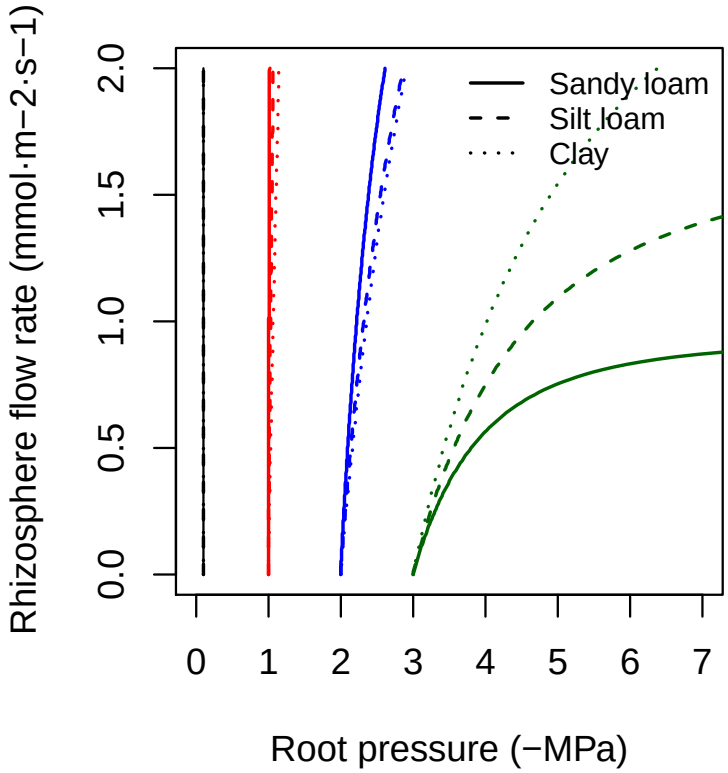

The nearly vertical lines indicate that for many values of E_i the corresponding drop in water potential through the rhizosphere will be very small. Only for increasingly negative soil water potential values the decrease in water potential through the rhizosphere becomes relevant. Both in the case of a xylem element or a rhyzosphere element the derivative $dE_i/d\Psi$ of the supply function is equal to the corresponding vulnerability curve.

1.2.2 Supply function of two elements in series

In the network of the two elements in series (rhizosphere + stem xylem) the supply function has to be calculated by sequentially using the previous supply functions. The E_i is identical for each element and equal to the canopy E. Since Ψ_{soil} is known, one first inverts the supply function of the rhizosphere to find Ψ_{root} (see `hydraulics.E2psiVanGenuchten()`) and then inverts the supply function of the xylem to find Ψ_{canopy} (see `hydraulics.E2psiXylem()`). The two operations can be summarized in a single supply function describing the potential rate of water supply for transpiration (E) as function of the canopy xylem pressure (Ψ_{canopy}), starting from different bulk soil (Ψ_{soil}) values (see `hydraulics.supplyFunctionTwoElements()`):

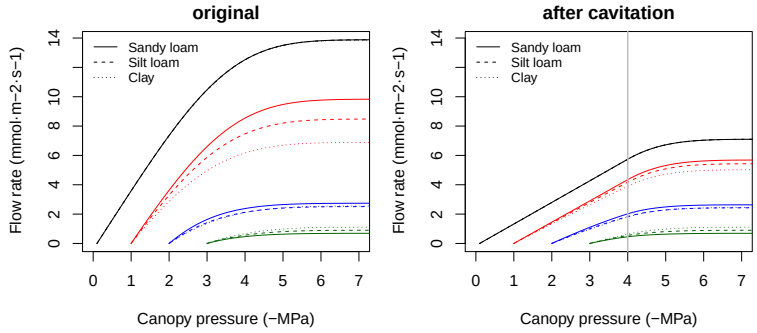

The supply function for the whole continuum contains much information. The Ψ intercept at $E = 0$ represents the predawn canopy sap pressure which integrates the rooted soil moisture profile. As E increments from zero, the disproportionately greater drop in Ψ_{canopy} results from the loss of conductance. As the soil dries the differences in flow due to soil texture become more apparent. The derivative of the whole continuum supply function, $dE/d\Psi$, is not equal to either of the vulnerability curves and it has to be obtained numerically. The derivative functions of the supply functions shown in the previous figure are:

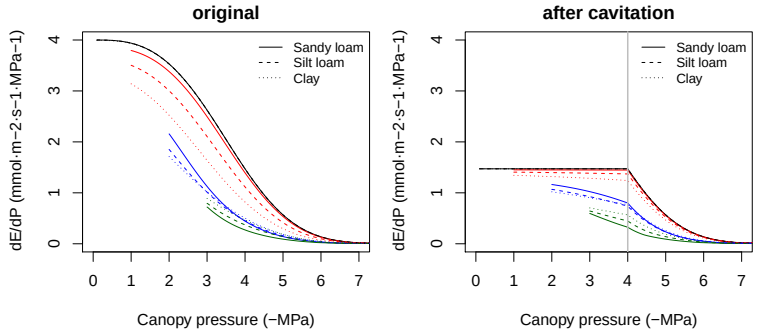

The derivative $dE/d\Psi_{canopy}$ is the conductance if the entire continuum was exposed to Ψ_{canopy} (Sperry & Love 2015). It corresponds to the local loss of hydraulic conductance at the downstream end of the flow path. It falls towards zero for asymptotic critical values (E_{crit}). For a cavitated system $dE/d\Psi_{canopy}$ can be rather flat, in accordance with the close to linear part of the supply function.

1.2.3 Supply function of a network

In an hydraulic network of N rhizosphere components and root layers in parallel there are $N + 1$ unknown pressures: the N root surface pressures $(\Psi_{rootsurf,1}, \ldots, \Psi_{rootsurf,N})$ and the root crown pressure at the downstream junction for all root components ($\Psi_{rootcrown}$). The $N+1$ unknown pressures are solved, for each specified total flow value E, using multidimensional

Newton-Raphson on a set of equations for steady-state flow (Sperry et al. 2016b):

$$E_{k,rhizosphere} - E_{k,root} = 0 \quad (5)$$

$$\sum_{k}^{n} E_{k,root} - E = 0 \quad (6)$$

where $E_{k,rhizosphere}$ and $E_{k,root}$ are calculated using either van Genuchten or Weibull function as vulnerability curves, respectively. In the case of rhizosphere elements, $\Psi_{up,k} = \Psi_{soil,k}$ and in the case of root elements $\Psi_{up,k} = \Psi_{rootsurf,k}$. Solving the steady-state equations also provides values for flow across each of the parallel paths $E_{k,rhizosphere} = E_{k,root}$, which are useful to conduct water balance operations on each layer. Canopy water potential is then obtained integrating the xylem vulnerability curve, using $\Psi_{up,k} = \Psi_{rootcrown}$ and assuming a steady-state flow E. The whole supply function $E(\Psi_{canopy})$ is obtained repeating these operations from $E = 0$ to a critical value E_{crit}.

As an example, we start by defining the water potential of three soil layers corresponding to four situations (analogously with the soil water potentials defined above):

```
>  psiSoilLayers1 = c(-0.3,-0.2,-0.1)
>  psiSoilLayers2 = c(-1.3,-1.2,-1.1)
>  psiSoilLayers3 = c(-2.3,-2.2,-2.1)
>  psiSoilLayers4 = c(-3.3,-3.2,-3.1)
```

In a network of several soil layers, one has to divide the total rhizosphere and root xylem conductances among layers. Let layer depths be:

```
> d = c(300,700,3000) #Soil layer widths in mm
```

Now let v_1, v_2 and v_3 be the proportion of fine root biomass in each soil layer.

```
> Z50 = 200 #Parameter of LDR root distribution
> Z95 = 1200 #Parameter of LDR root distribution
> v = root.ldrDistribution(Z50, Z95, d)
> v
```

```
          [,1]      [,2]       [,3]
[1,] 0.6652935 0.2749944 0.05971209
```

In the case of the rhizosphere conductances, we can simply define them (for each soil texture type) as:

```
> krhizomaxvec1 = krmax1*v
> krhizomaxvec2 = krmax2*v
> krhizomaxvec3 = krmax3*v
```

To divide maximum root xylem conductance among soil layers we need weights inversely proportional to the length of transport distances (Sperry et al. 2016b). Vertical transport lengths can be calculated from soil depths and radial spread can be calculated assuming cylinders with volume proportional to the proportions of fine root biomass. The whole process can be done using function `root.rootXylemConductanceProportions()`:

```
> weights = root.xylemConductanceProportions(v, d)
> weights
```

```
[1] 0.2369724 0.4214326 0.3415950
```

Transport weights are quite different than the fine root biomass proportions. This is because radial lengths are largest for the first (top) layer and vertical lengths are largest for the third (bottom) layer. The root xylem conductances are (in this case they do not depend on soil texture):

```
> krootmaxvec = krootmax*weights
> krootmaxvec
```

```
[1] 1.579816 2.809551 2.277300
```

Having all these maximum conductances, we can now build the supply functions for each soil texture and starting from the different soil water potential configurations (see `hydraulics.supplyFunctionNetwork()`):

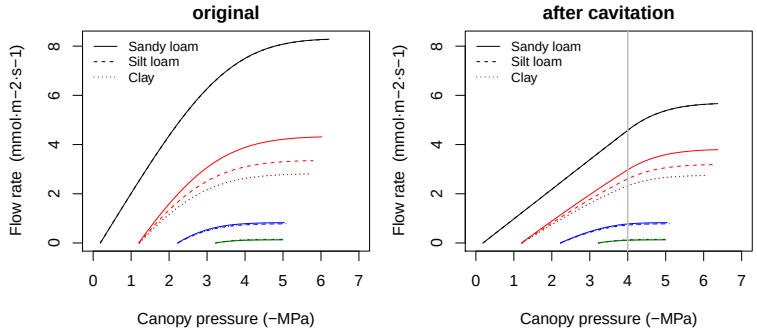

As with the two-element case, the derivative of $dE/d\Psi_{canopy}$ for the network topology is obtained numerically:

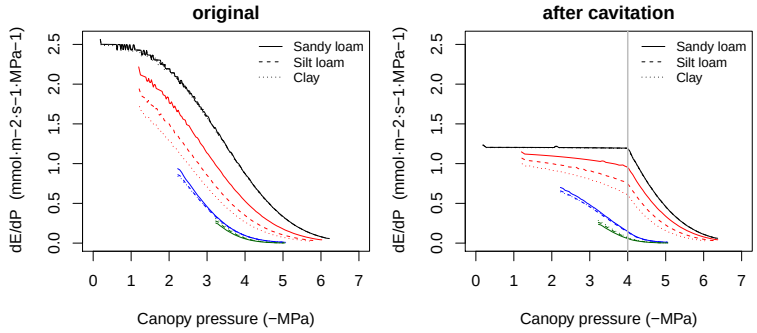

Although it is computationally more expensive, an advantage of working with the network is that we can know the water potentials in different points of the continuum. Here we plot them for the results of silt loam texture and the four soil potential vectors defined above:

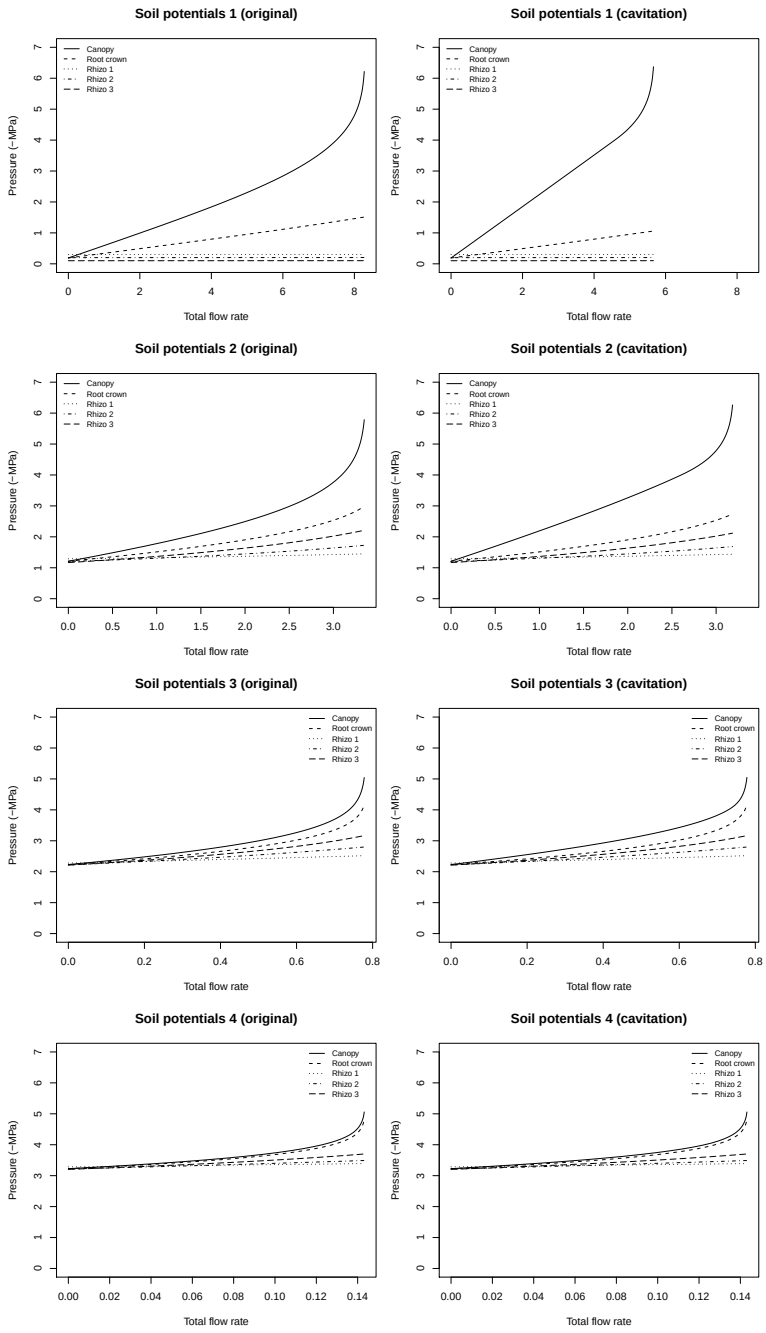

Note that when soil is not dry (first situation) pressure drop in the rhizosphere is negligible, but not the pressure drop in the root xylem. For drier

soils rhizosphere becomes more relevant.

In a network with resistance elements in parallel, we can also know the flow rates across each of the parallel paths (again corresponding to the results of silt loam texture and for the four soil potential vectors):

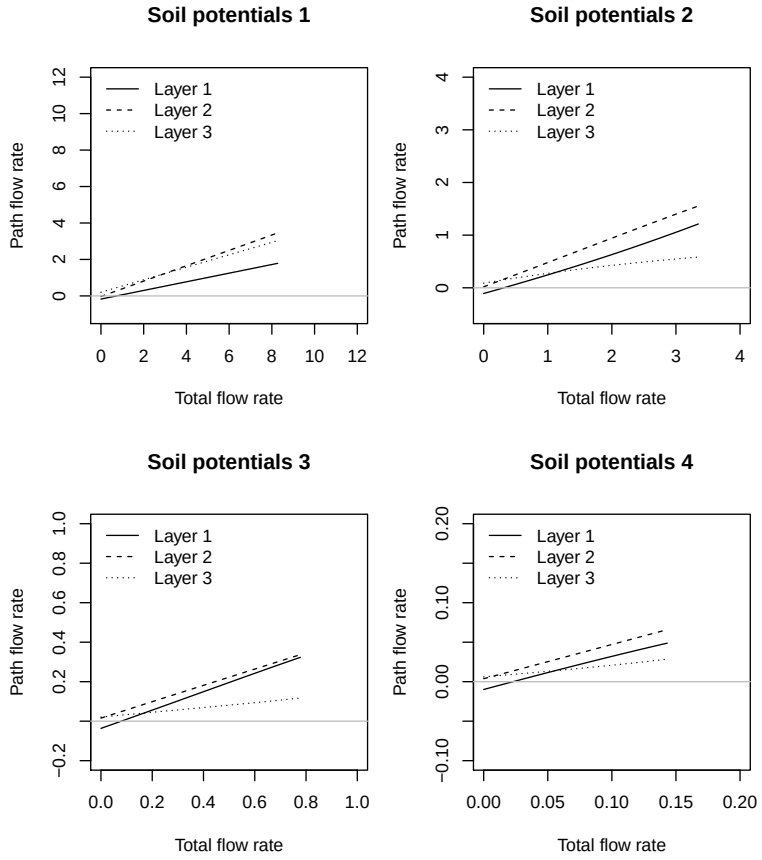

Note that the contribution of each soil layer depends on the soil conditions and the total amount of flow. for low total flow rates some layers may have negative flows if their potential is lower than others, indicating hydraulic redistribution.

2 Leaf VPD, conductance to water vapor and photosynthesis

The water supply function can be translated into a photosynthesis function (Sperry et al. 2016b). In a nutshell, E from the supply function is used to calculate leaf temperature and leaf water vapor deficit from energy balance. The diffusive conductances of the leaf to water and CO2 are obtained from water supply and water vapor deficit. The gross assimilation

rate is then obtained from the diffusive conductance and a modelled curve between assimilation and leaf internal CO2 concentration. Gross assimilation is calculated, without subtracting autotrophic respiration, the purpose is to represent the instantaneous gain of opening the stomata.

2.1 Leaf temperature and vapor pressure deficit

Leaf temperature (T_{leaf}; in Celsius) can be calculated for any given flow rate $E(\Psi_{leaf})$ using (Campbell and Norman 1998):

$$T_{leaf}(\Psi_{leaf}) = T_{air} + \frac{I_{nsw} - \epsilon \cdot \sigma \cdot (T_{air} + 273.15)^2 - \lambda_v \cdot E(\Psi_{leaf})}{C_p \cdot (g_r + g_{Ha})} \quad (7)$$

where I_{nsw} (in $W \cdot m^{-2}$) is the instantaneous shortwave radiation absorbed by the leaves expressed per leaf area units (should include longwave radiation), $E(\Psi_{leaf})$ is the flow (converted to $mol \cdot s^{-1} \cdot m^{-2}$ per two-sided leaf area basis),ϵ is emissivity (0.97), σ is the Stephan-Boltzman constant, T_{air} is the air temperature (in ºC), $C_p = 29.3 J \cdot mol^{-1} \cdot C^{-1}$ is the specific heat capacity of dry air at constant pressure and λ_v is the latent heat of vaporization (in $J \cdot mol^{-1}$):

$$\lambda_v = (2.5023 \cdot 10^6 - (2430.54 \cdot T_{air})) \cdot 0.018 \quad (8)$$

Finally, g_r and g_{Ha} are the radiative and heat conductance values ($mol \cdot m^{-2} \cdot s^{-1}$), respectively (Campbell and Norman 1998):

$$g_r = \frac{4 \cdot \epsilon \cdot \sigma (T_{air} + 273.15)^3}{C_p} \quad (9)$$

$$g_{Ha} = 0.189 \cdot (u/d)^{0.5} \quad (10)$$

where u is wind speed (in $m \cdot s^{-1}$), taken as the wind speed at mid-crown height, and d is the 0.72 times the leaf width (here 0.01 m).

The following figure illustrates the value of T_{leaf} for varying values of wind speed and flow rate, calculated for the following air temperature and instantaneous absorved radiation:

```
> Tmin = 15
> Tmax = 30
> Tair = meteoland::utils_averageDaylightTemperature(Tmin, Tmax)
> Tair

[1] 24.09

> Rabs = 740 #W * m-2
```

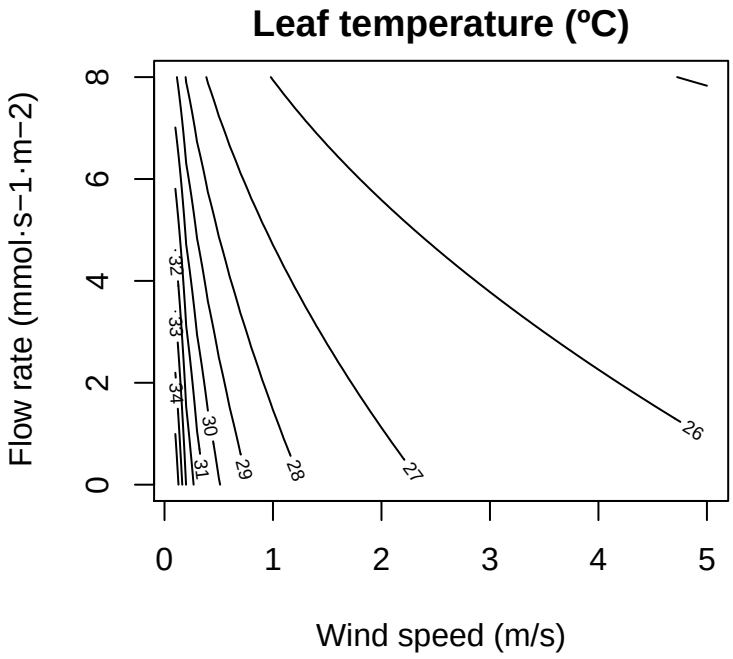

Let's assume that wind speed is 2 m/s. The application of the above equations to the $E(\Psi_{leaf})$ curves corresponding to the complete hydraulic network yields the following $T_{leaf}(\Psi_{leaf})$ curves:

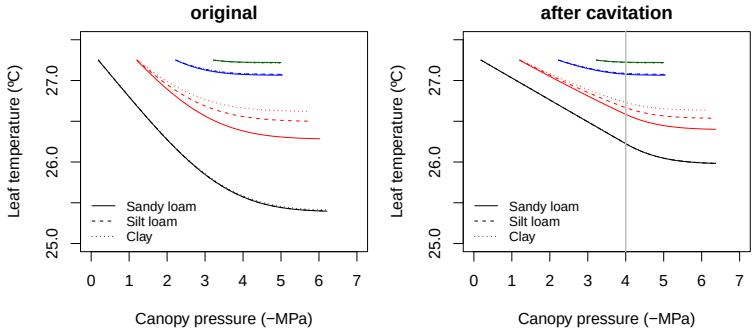

Thus, transpiration decreases leaf temperature (whereas radiation increases it and wind speed makes it more similar to air temperature). Vapor pressure deficit in the leaf (VPD_{leaf}, in kPa) is calculated as:

$$VPD_{leaf} = VP(T_{leaf}) - vp_{day} \tag{11}$$

Where vp_{day} is the average daily vapor pressure and $VP(T)$ is a function giving the saturated vapor pressure for temperature T. Let us assume the following values of relative humidity, yielding an average vp_{day}:

```
> RHmin = 60
> RHmax = 75
```

```
> vpa = utils_averageDailyVP(Tmin, Tmax, RHmin, RHmax)
> vpa

[1] 1.912181
```

the application of the above equation to the $T_{leaf}(\Psi_{leaf})$ curves yields the following $VPD_{leaf}(\Psi_{leaf})$ curves:

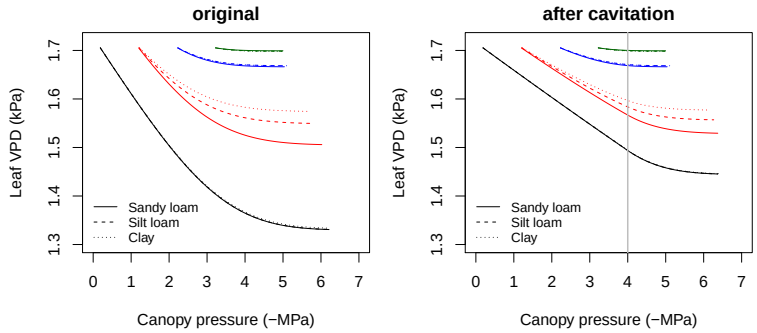

Since leaf VPD increases with leaf temperature, transpiration decreases leaf VPD.

2.2 Leaf conductance to water vapor

Leaf conductance to water vapor (g_{sw}; in $molH_2O \cdot s^{-1} \cdot m^{-2}$) and to carbon dioxide (g_{sc}; in mol $CO^2 \cdot s^{-1} \cdot m^{-2}$) are obtained for each value of E and VPD_{leaf} using:

$$g_{sw} = E \cdot \frac{P_{atm}}{VPD_{leaf}} \quad (12)$$

$$g_{sc} = g_{sw}/1.6 \quad (13)$$

the application of the equation for g_{sw} to the $VPD_{leaf}(\Psi_{leaf})$ curves yields the following $g_{sw}(\Psi_{leaf})$ curves:

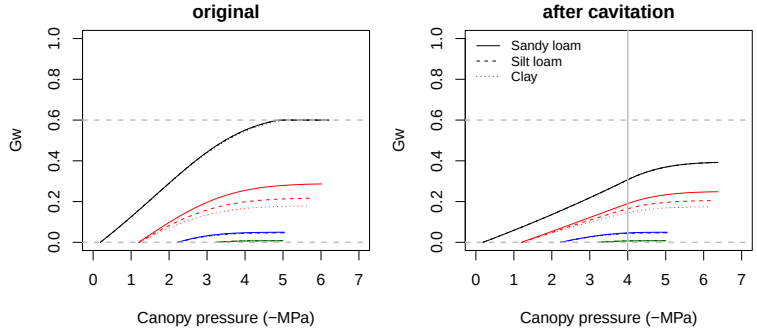

Hence, larger values of transpiration require larger values of leaf water vapour conductance. In the previous figure we have indicated the thresholds of g_{swmin} and g_{swmax}, the species-specific minimum and maximum water vapour conductances (i.e. conductances when stomata are fully closed and fully open, respectively).

```
> Gmin = 0.00001;
> Gmax = 0.6
```

g_{sw} cannot exceed g_{swmax} so that some flow rates may not be possible (see stomatal regulation below). However, g_{swmax} should quickly become non-limiting as soil dries (i.e. reducing E) or VPD_{leaf} increases (Sperry et al. 2016a).

2.3 Leaf photosynthesis

Rubisco-limited photosynthesis rate A_c (in $\mu molCO_2 \cdot s^{-1} \cdot m^{-2}$) was obtained from (Collatz et al. 1991, Medlyn et al 2002):

$$A_c = \frac{V_{max} \cdot (C_i - \Gamma*)}{C_i + K_c \cdot (1 + O_a/K_o)} \tag{14}$$

where V_{max} is Rubisco's maximum carboxylation rate (in $\mu molCO_2 \cdot s^{-1} \cdot m^{-2}$), C_i is the internal carbon dioxide concentration (in $\mu mol \cdot mol^{-1}$), $\Gamma*$ is the compensation point (in $\mu mol \cdot mol^{-1}$), K_c (in $\mu mol \cdot mol^{-1}$) and K_o (in $mmol \cdot mol^{-1}$) are Michaelis-Menten constants for carboxylation and oxygenation, respectively, and O_a is the atmospheric oxygen concentration (i.e. $209 mmol \cdot mol^{-1}$). $\Gamma*$, K_c and K_o depend on leaf temperature (T_{leaf}, in Celsius) (Bernacchi et al. 2001):

$$\Gamma* = 42.75 \cdot e^{\frac{37830 \cdot (T_{leaf} - 25)}{298 \cdot R \cdot (T_{leaf} - 273)}} \tag{15}$$

$$K_c = 404.9 \cdot e^{\frac{79430 \cdot (T_{leaf} - 25)}{298 \cdot R \cdot (T_{leaf} - 273)}} \tag{16}$$

$$K_o = 278.4 \cdot e^{\frac{36380 \cdot (T_{leaf} - 25)}{298 \cdot R \cdot (T_{leaf} - 273)}} \tag{17}$$

Electron transport-limited photosynthesis A_e (in $\mu molCO_2 \cdot s^{-1} \cdot m^{-2}$) was obtained from Medlyn et al. (2002):

$$A_e = \frac{J}{4} \cdot \frac{C_i - \Gamma*}{C_i + 2 \cdot \Gamma*} \tag{18}$$

$$J = \frac{(\alpha \cdot Q + J_{max}) - \sqrt{(\alpha \cdot Q + J_{max})^2 - 4.0 \cdot c \cdot \alpha \cdot Q \cdot J_{max}}}{2 \cdot c} \tag{19}$$

where α is the quantum yield of electron transport (0.3 mol electrons·mol photons^{-1}), Q is the PAR photon flux density (μmol photons·$m^{-2} \cdot s^{-1}$), which is calculated from leaf irradiance (I_{par}; in $W \cdot m^{-2}$):

$$Q = I_{par} \cdot 546 \cdot 0.836 \cdot 10^{-2} \tag{20}$$

J_{max} and J are the maximum and actual rate of electron transport (both in μmol electrons$\cdot m^{-2} \cdot s^{-1}$) and $c = 0.9$ defines the curvature of the light-response curve. The gross assimilation rate A at a given C_i is the minimum of A_e and A_c. To obtain a smooth A-vs-C_i curve we used (Collatz et al. 1991):

$$A = \frac{(A_c + A_e) - \sqrt{(A_c + A_e)^2 - 4.0 \cdot c' \cdot A_e \cdot A_c}}{2 \cdot c'} \tag{21}$$

where $c' = 0.98$ is a curvature factor. The temperature dependence of J_{max} and V_{max} relative to 25^{o}C was modelled using Leuning (2002) (his eq. 1 with parameters from his Table 2). The internal CO_2 concentration, C_i, needs to be known to calculate A using the previous equations. Sperry et al. (2016b) use a second equation for A which uses g_{cs}:

$$A = g_{sc} \cdot (C_{atm} - C_i) \tag{22}$$

where C_{atm} is the atmospheric CO_2 concentration. Combining the two equations for A and finding the root of the resulting equation using Newton-Raphson method allows determining C_i and therefore A. Thus, after defining PAR photon flux density, atmosphere CO_2 concentration and maximum rate parameters:

```
> Q = 2000
> Catm = 386
> Vmax298 = 100
> Jmax298 = 1.67*Vmax298
```

one can obtain the following $A(\Psi_{leaf})$ curves from $T_{leaf}(\Psi_{leaf})$ and $g_{sc}(\Psi_{leaf})$:

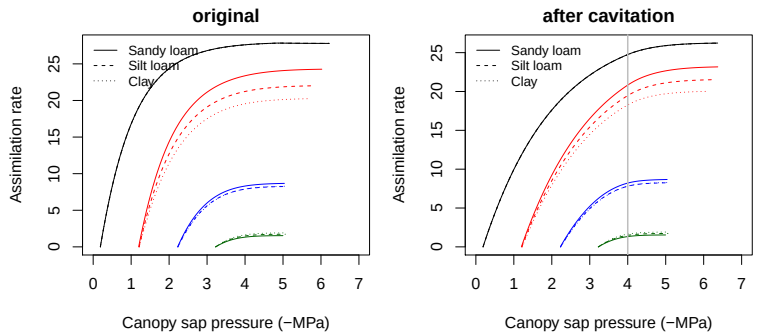

2.4 Canopy photosynthesis

In the previous subsection far we calculated photosynthesis at the leaf level. However, the function $A(\Psi_{leaf})$ can be calculated for a whole canopy. Essentially we need to repeat the calculations of leaf temperature, leaf VPD, leaf gas conductance and photosynthesis for every leaf to be considered in the canopy. Gross and net photosyntehsis values can be then aggregated

across the canopy for each value of Ψ_{leaf}, so that the function $A(\Psi_{leaf})$ is obtained. Here we will consider a canopy of one species divided into 10 layers, with constant leaf density:

```
> LAI = 2
> nlayer = 10
> LAIlayerlive = matrix(rep(LAI/nlayer,nlayer),nlayer,1)
> LAIlayerdead = matrix(0,nlayer,1)
> kb = 0.8
> kd_PAR = 0.5
> kd_SWR = kd_PAR/1.35
> alpha_PAR = 0.9
> gamma_PAR = 0.04
> gamma_SWR = 0.05
> alpha_SWR = 0.7
```

Many aspects may vary across the canopy, including environmental conditions (such as direct/diffuse light or wind speed) and photosynthesis parameters (e.g. Vmax298). The previous canopy definition and light parameters lead to a percentage of the above-canopy irradiance reaching each layer (Goudriaan 2016; Anten and Bastiaans 2016). Furthermore, it is generally accepted that sunlit and shade leaves need to be treated separately (De Pury and Farquhar 1997). Extinction of direct radiation also defines the proportion of leaves of each layer that are affected by direct light beams (i.e. the proportion of sunlit leaves).

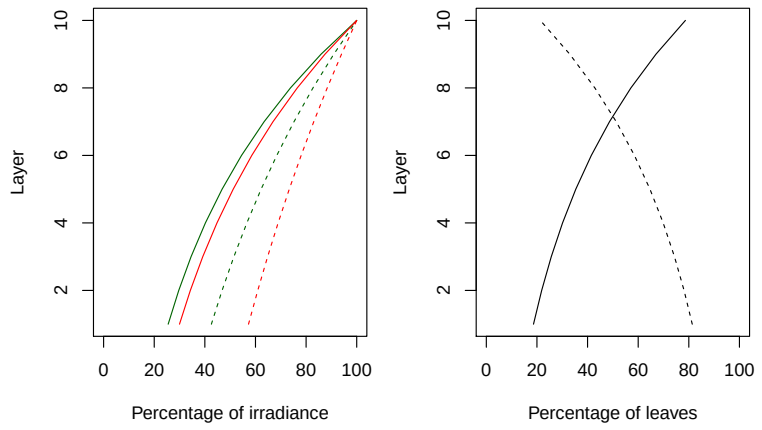

For simplicity, here we will assume constant windspeed in all layers:

```
> ulayer = rep(2, 10)
```

Regarding incoming light, we assume the following direct and diffuse irradiance at the top of the canopy:

```
> solarElevation = 0.67
> SWR_direct = 1100
> SWR_diffuse = 300
> PAR_direct = 550
> PAR_diffuse = 150
```

Solar elevation is the angle between the sun and the horizon (i.e. the complement of the zenith angle). Under these conditions, the amount of shortwave and PAR radiation absorbed per unit of leaf area at each canopy layer is (Anten and Bastiaans 2016):

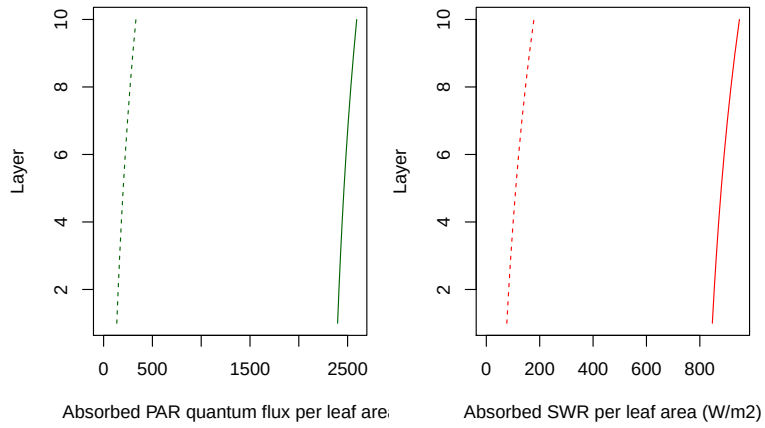

Following De Pury and Farquhar (1997), we further assume that maximum assimilation rates are highest for leaves at the top of the canopy and there is a exponential decrease from there towards the bottom, where maximum rates are 50% of those at the top:

$$V_{max,298}(L_i) = V_{max,298} \cdot exp(-0.713 \cdot L_i/LAIc) \tag{23}$$

where L_i is the cumulative LAI value at a given canopy layer i and $LAIc$ is the canopy LAI.

Multilayer canopy models allow evaluating leaf conditions, stomatal conductance and photosynthesis for different points of the canopy. However, this comes at high computational cost. While big-leaf canopy models are known to be unaccurate under some situations, sun-shade canopy models (De Pury and Farquhar 1997) provide estimates that are close to multiple layer models (Hikosaka 2016). Sun-shade models involve: (a) aggregating the leaf area of sunlit/shade leaves across layers; (b) aggregating the light absorbed by leaves of each kind across layers; and (c) aggregating maximum assimilation rates across layers, again separating sunlit and shade leaves. One then calls the photosynthesis model twice (i.e. once for shade leaves and once for sunlit leaves), using the aggregated maximum assimilation rates. Separating the two kinds of leaves acknowledges that they operate at different

parts of the light-saturation curve. The following figure provides the canopy photosynthesis functions obtained, under different situations, using a full 10-layer canopy description (top), a sunshade canopy model (center) or a big-leaf model (bottom). Note the coincidence between the multi-layer and the sun-shade models.

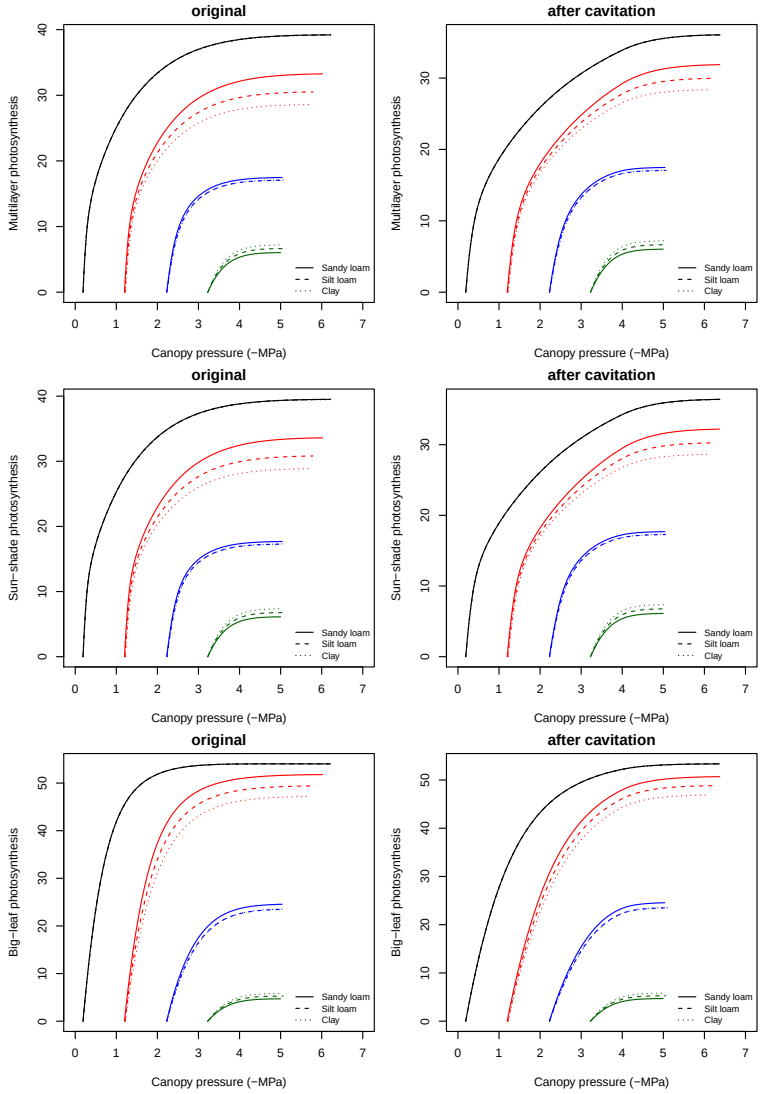

3 Stomatal regulation by profit maximization

3.1 Cost and gain functions

The hydraulic supply function is used to derive a transpirational *cost function* $\theta_1(\Psi_{leaf})$ that reflects the increasing damage from cavitation and the

greater difficulty of moving water along the continuum (Sperry et al. 2016b):

$$\theta_1(\Psi_{leaf}) = \frac{k_{cmax} - k_c(\Psi_{leaf})}{k_{cmax} - k_{crit}} \tag{24}$$

where $k_c(\Psi_{leaf}) = dE/d\Psi(\Psi_{leaf})$ is the slope of the supply function, $k_{cmax} = dE/d\Psi(\Psi_{soil})$ and $k_{crit} = dE/d\Psi(\Psi_{crit})$ is the slope of the supply function at $E = E_{crit}$ the critical flow beyond which hydraulic failure occurs.

Alternatively, we considered two additional cost functions ($\theta_2(\Psi_{leaf})$ and $\theta_3(\Psi_{leaf})$) using the vulnerability curve of the xylem:

$$\theta_2(\Psi_{leaf}) = \frac{k_{xmax} - k_x(\Psi_{leaf})}{k_{xmax}} \tag{25}$$

$$\theta_3(\Psi_{leaf}) = \frac{k_{xmax} - k_{xcav}(\Psi_{leaf})}{k_{xmax}} \tag{26}$$

where k_x and k_{xcav} are the xylem conductance function before and after irreversible cavitation, respectively; and and k_{xmax} is the maximum conductance value. Using the xylem vulnerability curve for the cost function is grounded on the fact that stomatal regulation occurs at leaves, so that regulation should respond to the loss of hydraulic conductance at this point, independently of what happens to the rest of the continuum. Obviously, θ_2 and θ_3 are the same before irreversible cavitation. The difference between them may be interpreted as the following. While θ_2 strictly follows the potential at the leaf level (and hence could be related to a loss of turgor), independently of what happened upstream, θ_3 would sense the previous loss of conductance in the xylem.

The following figures illustrate the θ_1, θ_2 and θ_3 curves corresponding to the supply and assimilation functions:

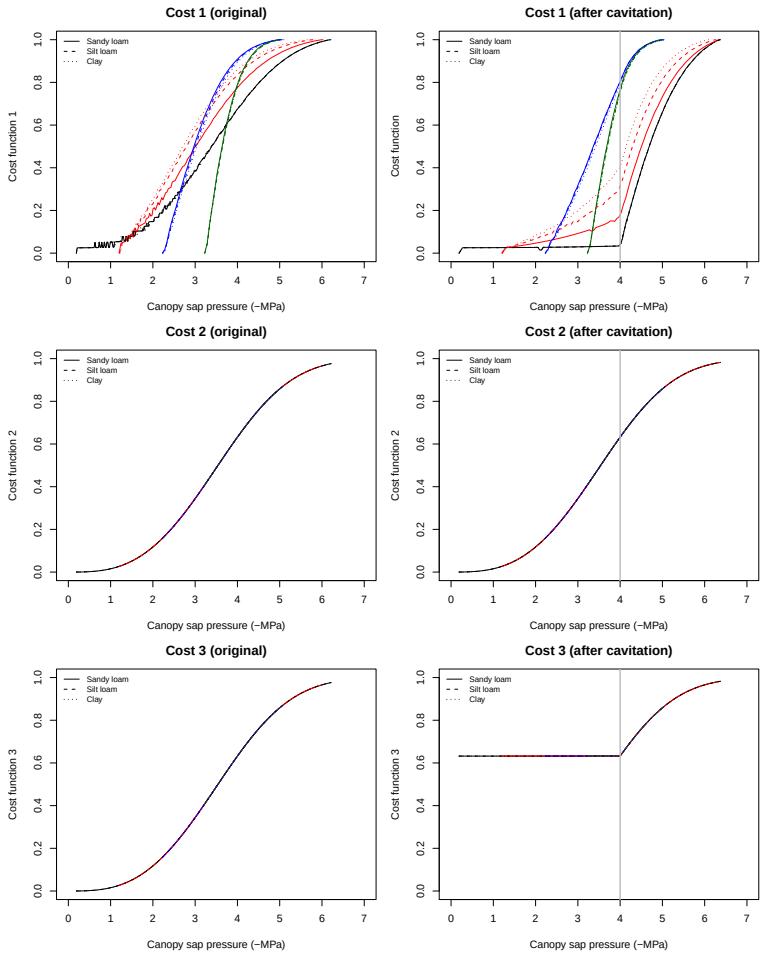

The normalized photosynthetic *gain function* $\beta(\Psi_{leaf})$ reflects the actual assimilation rate with respect to the maximum:

$$\beta(\Psi_{leaf}) = \frac{A_n(\Psi_{leaf})}{A_{nmax}} \tag{27}$$

where A_{nmax} is the instantaneous maximum assimilation rate estimated over the full Ψ_{leaf} range.

The following figures illustrate the $\theta(\Psi_{leaf})$ and $\beta(\Psi_{leaf})$ curves corresponding to the supply and assimilation functions:

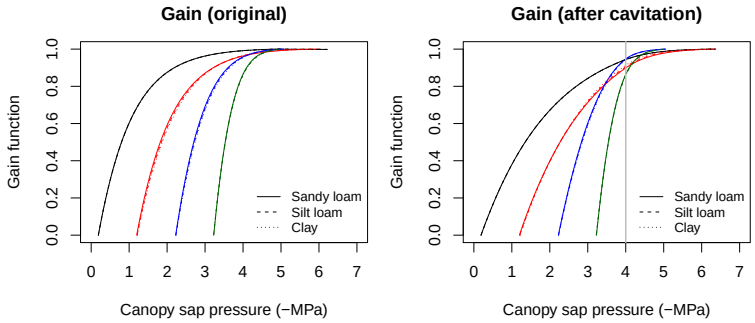

3.2 Profit maximization

According to Sperry et al (2016b), stomatal regulation can be effectively estimated by determining the maximum of the *profit function* ($Profit(\Psi_{leaf})$), for which we consider three alternatives corresponding to the three cost functions:

$$Profit_1(\Psi_{leaf}) = \beta(\Psi_{leaf}) - \theta_1(\Psi_{leaf}) \quad (28)$$

$$Profit_2(\Psi_{leaf}) = \beta(\Psi_{leaf}) - \theta_2(\Psi_{leaf}) \quad (29)$$

$$Profit_3(\Psi_{leaf}) = \beta(\Psi_{leaf}) - \theta_3(\Psi_{leaf}) \quad (30)$$

Once Ψ_{leaf} that maximizes profit is determined, the values of the remaining variables are also determined. At this point, it may happen that $g_{sw}(\Psi_{leaf})$ is lower than the minimum (i.e. cuticular) water vapor conductance (g_{swmin}) or larger than the maximum water vapor conductance (g_{swmax}). These thresholds need to be taken into account when determining the maximum of the profit function. The following figures illustrate the $Profit_1(\Psi_{leaf})$, $Profit_2(\Psi_{leaf})$ and $Profit_3(\Psi_{leaf})$ curves of corresponding to the previous cost and gain curves:

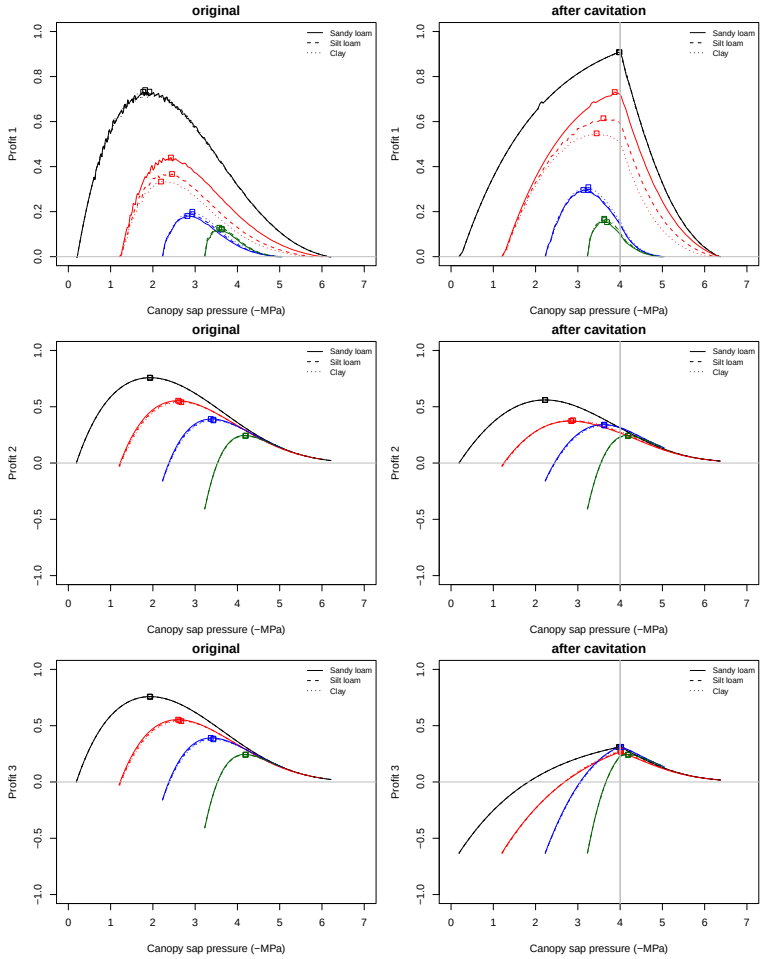

Squares in the previous figures indicate the maximum profit points in each situation. In the case of non-cavitated system (left panels), the drier the soil, the closer is the maximum profit Ψ_{leaf} to soil water potential as one would expect intuitively. This occurs for all three profit functions. Unlike θ_1 which is different for each soil texture (and soil potential), θ_2 and θ_3 are the same for all soil textures. As a result, the regulation points do not differ much among textures in $Profit_2$ and $Profit_3$ because the only difference is in the gain function. For a system with xylem cavitation (right panel), the maximum $Profit_1$ curves behave strangely. In particular may get a more negative value for Ψ_{canopy} for wet soils than for dry soils. This effect does not occur when using either $Profit_2$ or $Profit_3$. The difference between them is that $Profit_3$ brings all regulated potentials close to the value that caused irreversible cavitation (assuming that operating at lower potentials does not have advantage because cavitation has already occurred). $Profit_2$ does not have this effect, although it still brings plant water potentials to more negative values after cavitation. Although cavitation did not change the θ_2 function, the supply function is flatter and this affects the gain function,

making it increase less steeply with lower potentials.

Differences between profit functions can be more easily seen when plotting the change from original (uncavitated) regulation to the cavitated one, in terms of both canopy sap pressure and flow rate:

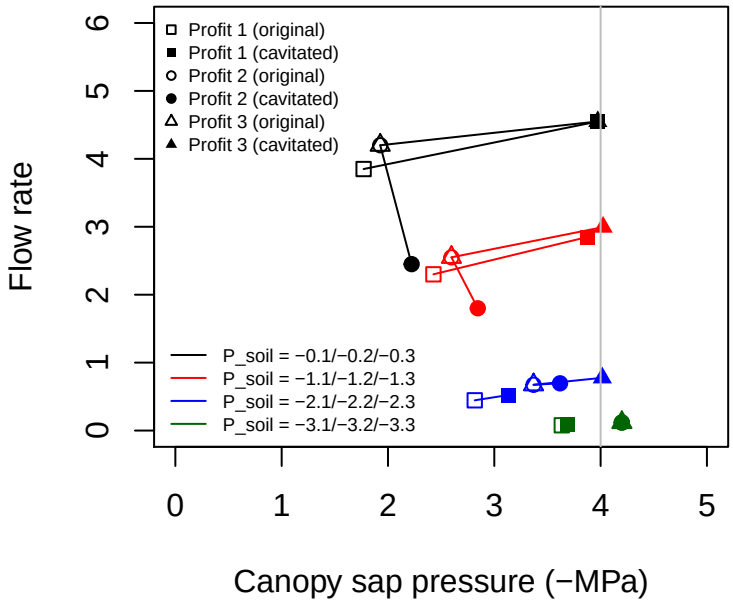

In both $Profit_1$ and $Profit_2$ irreversible cavitation often brings, after soil rewetting, less conservative stomatal regulation that enables higher flow rates. This does not seem to happen in $Profit_2$, where despite irreversible cavitation leads to more negative water potentials the reduction, predicted flow rates after rewetting are not above those predicted before cavitation.

3.3 Stomatal regulation for combinations of environmental cues

The following figures illustrate the behavior of stomatal regulation by profit maximization under different combination of light levels (from 0% to 100% of absorbed SWR and PAR) and soil water potential (from 0 to -4 MPa). In these calculations we are using $Profit_2$ as function for profit maximization.

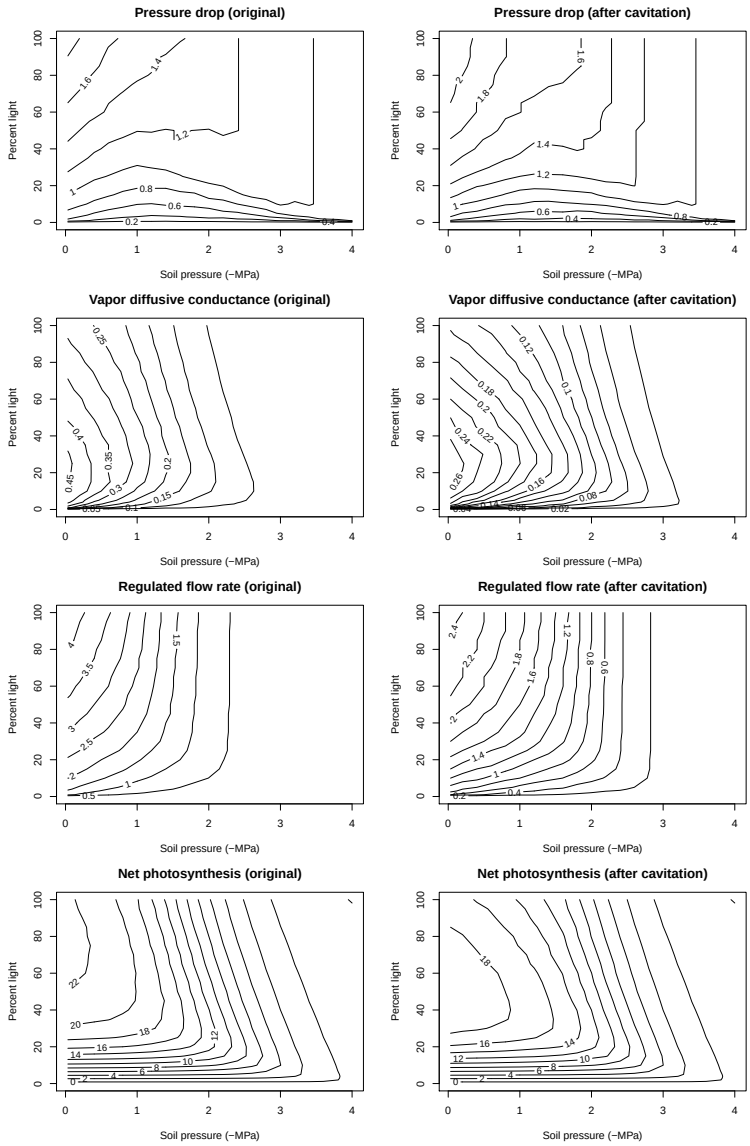

As expected, canopy pressure drop, regulated flow rates and net photosynthesis are largest for high levels of light and low levels of soil water deficit. Decreases of light availability or increases of soil water deficit lead to a decrease in these three variables. Net photosynthesis (i.e. after accounting for autotrophic respiration) can be negative for dry soils (or very low levels of light).

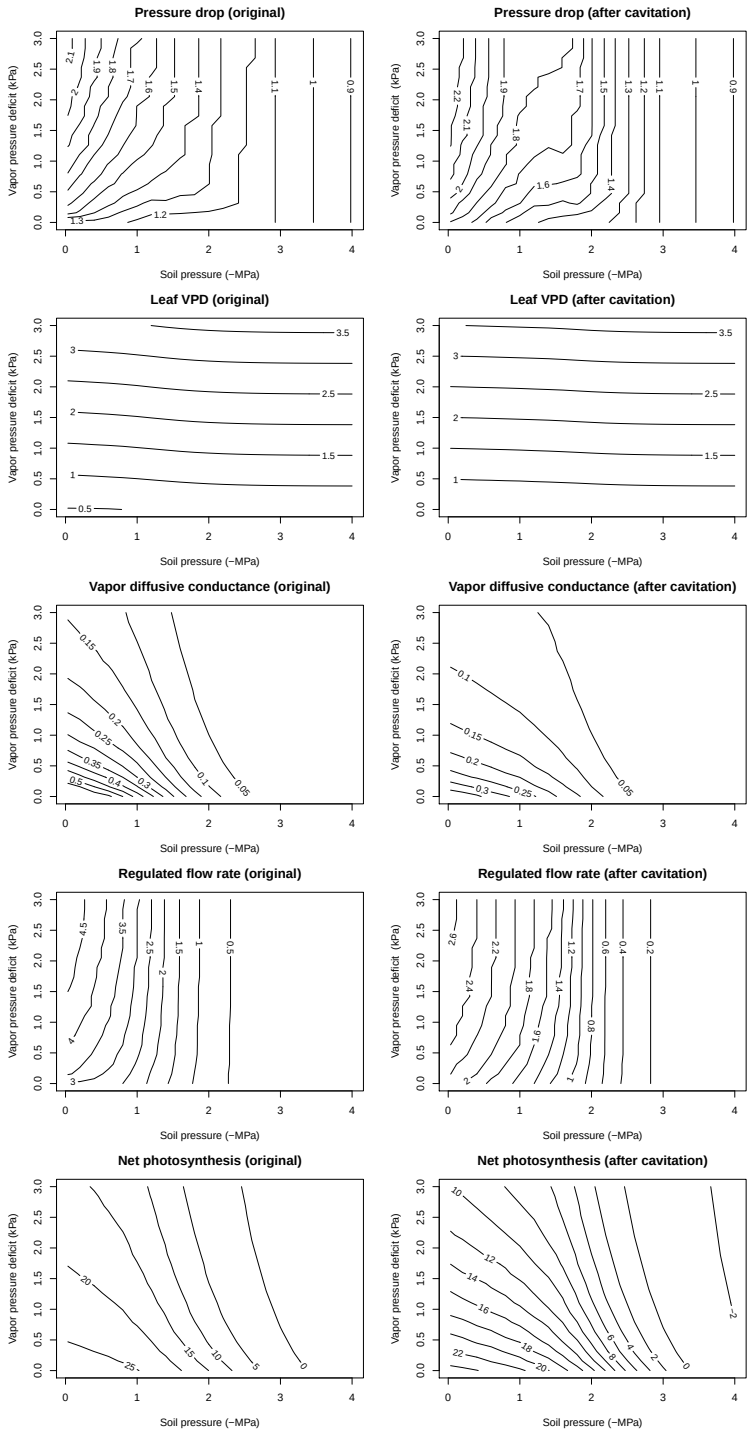
Pressure drop (original)
Pressure drop (after cavitation)
Leaf VPD (original)
Leaf VPD (after cavitation)
Vapor diffusive conductance (original)
Vapor diffusive conductance (after cavitation)
Regulated flow rate (original)
Regulated flow rate (after cavitation)
Net photosynthesis (original)
Net photosynthesis (after cavitation)
Vapor pressure deficit (kPa)
Soil pressure (−MPa)

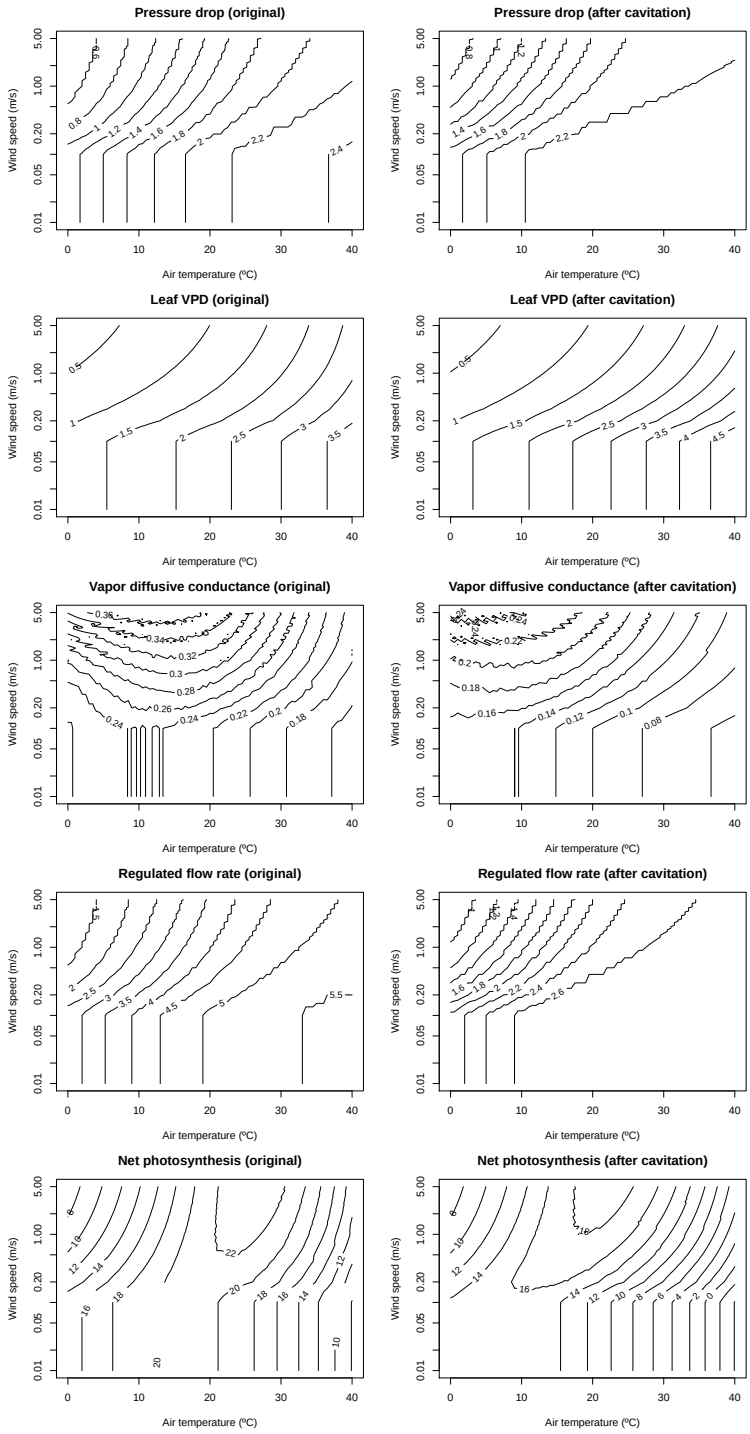
Pressure drop (original)
Pressure drop (after cavitation)
Leaf VPD (original)
Leaf VPD (after cavitation)
Vapor diffusive conductance (original)
Vapor diffusive conductance (after cavitation)
Regulated flow rate (original)
Regulated flow rate (after cavitation)
Net photosynthesis (original)
Net photosynthesis (after cavitation)
Wind speed (m/s)
Air temperature (ºC)

4 References

- Bernacchi, C. J., E. L. Singsaas, C. Pimentel, A. R. Portis, and S. P. Long. 2001. Improved temperature response functions for models of Rubisco-limited photosynthesis. Plant, Cell and Environment 24:253–259.

- Campbell, G. S., and J. M. Norman. 1998. An introduction to environmental biophysics. 2nd edition.

- Collatz, G. J., J. T. Ball, C. Grivet, and J. A. Berry. 1991. Physiological and environmental regulation of stomatal conductance, photosynthesis and transpiration: a model that includes a laminar boundary layer. Agricultural and Forest Meteorology 54:107–136.

- De Pury, D.G.G. and Farquhar, G.D. 1997. Simple scaling of photosynthesis from leaves to canopies without the errors of big-leaf models. Plant, Cell and Environment, 20, 537–557.

- Medlyn, B. E., E. Dreyer, D. Ellsworth, M. Forstreuter, P. C. Harley, M. U. F. Kirschbaum, X. Le Roux, P. Montpied, J. Strassemeyer, A. Walcroft, K. Wang, and D. Loustau. 2002. Temperature response of parameters of a biochemically based model of photosynthesis. II. A review of experimental data. Plant, Cell and Environment 25:1167–1179.

- Sperry, J. S., F. R. Adler, G. S. Campbell, and J. P. Comstock. 1998. Limitation of plant water use by rhizosphere and xylem conductance: results from a model. Plant, Cell & Environment 21:347–359.

- Sperry, J. S., and D. M. Love. 2015. What plant hydraulics can tell us about responses to climate-change droughts. New Phytologist 207:14–27.

- Sperry, J. S., Y. Wang, B. T. Wolfe, D. S. Mackay, W. R. L. Anderegg, N. G. McDowell, and W. T. Pockman. 2016a. Pragmatic hydraulic theory predicts stomatal responses to climatic water deficits. New Phytologist 212:577–589.

- Sperry, J. S., M. D. Venturas, W. R. L. Anderegg, M. Mencuccini, D. S. Mackay, Y. Wang, and D. M. Love. 2016b. Predicting stomatal responses to the environment from the optimization of photosynthetic gain and hydraulic cost. Plant Cell and Environment.